Magnets, Superconductors and Cryostats
TE-MSC

March 2013
Internal Note 2013-10
EDMS Nr: 1266788

Results of the first measuring campaign of the Daresbury Permanent Magnet High Gradient Quadrupole Prototype for the CLIC Drive Beam

Authors: Antonio Bartalesi, Michele Modena, Michael Struik.

Keywords: CLIC, Permanent Magnet, Quadrupole, Gradient, Axis Stability.

Abstract

This report contains the results of the measuring campaign performed on the Daresbury Laboratory CLIC Drive Beam Quadrupole prototype (DBQ-PM); a tunable quadrupole entirely based on permanent magnets.

1. Introduction

In the frame of the CLIC-UK Collaboration between Daresbury Laboratory and CERN, a prototype of the CLIC Drive Beam Permanent Magnet Quadrupole (DBQ-PM) designed and procured by Daresbury Lab., was shipped to CERN to perform the following measurements:

1. Maximum achievable integrated gradient,
2. Characteristic curve (integrated gradient values in the whole tunable range),
3. Magnetic field quality at different gradients,
4. Magnetic axis stability of the DBQ-PM at different gradients.

When the DBQ-PM was delivered to CERN, it was possible to cover all of the points listed above in a first measuring campaign, apart from the field quality, for which it is necessary either a rotating coil or a vibrating wire measuring technique, that were not available at the time.

2. Magnetic measurements

This campaign started by measuring the integrated gradient, characteristic curve and axis displacement with the Stretched Wire (SW) technique. The magnet was transported to the Magnetic Measurement Lab. in I8, where it was measured with the help of the colleagues from the TE-MSC/MM Section, who also provided the necessary space and instrumentation.

2.1. Measurements set-up

The stretched wire measurements were performed on the CERN `SSW-1` station. This system has an estimated precision for the determination of the magnetic axis of $\pm 5\,\mu m$. Figure 1 shows the magnet on the stretched wire bench, ready to be measured.

2.2. Cycle followed

The DBQ-PM was set at several different gradients, for a total of 21 subsequent steps, and two magnetic measurements were performed at each stage.
For this measuring cycle it was decided to start from the maximum gradient, achieved when the DBQ-PM permanent magnet blocks are as close as possible to the poles; and then move outward the permanent magnets in order to decrease the gradient, until reaching the maximum distance that the slide is allowed to travel by the mechanics, to reach the minimum gradient. During this cycle, the slide movement was interrupted at given values of distance, to perform the magnetic measurements.
After passing from the maximum to the minimum gradient configuration, with a total

Figure 1: stretched wire measurements set-up.

of 14 intermediate values; the permanent magnets were moved from the farther to the closest position repeatedly for three times, to evaluate the repeatability of the magnetic performances over a wide operational range.

2.3. Magnetic measurements results and conclusions

The results of the integrated gradient measurements, obtained during the cycle described above, are represented in figure 2. In this plot there are two series of values almost overlapped, as the integrated gradient is measured separately in the x and y planes. The following signs convention is adopted: the z axis lays on the beam line, while the y and the x axis are respectively perpendicular and parallel to the ground.
With a value of 14.5 T achieved in both the x and the y axes, it was *confirmed* that the DBQ-PM is able to develop the required integrated gradient.
The characteristic curve shown in figure 3 is obtained by relating the integrated gradient with the magnet setting position, given by the PM blocks displacement.
The following plot (figure 4) shows the displacement of the magnetic axis in the x and y directions, during consequent measurements. A visual correlation with the integrated

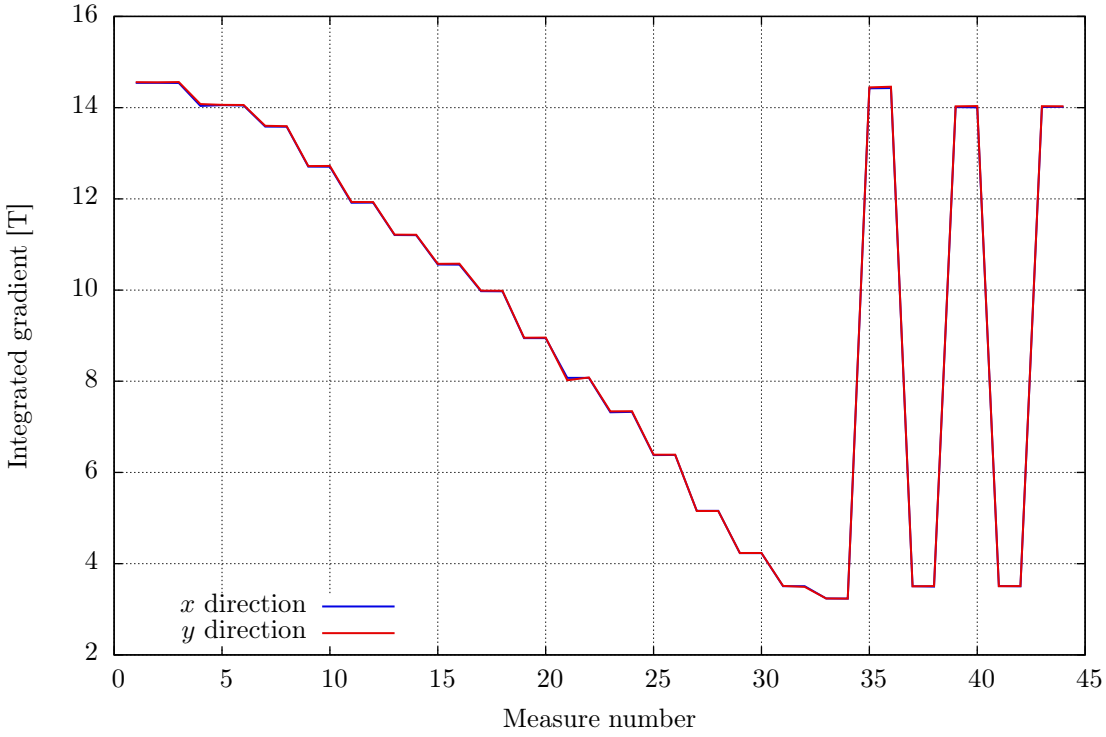

Figure 2: integrated gradients during the whole measuring cycle.

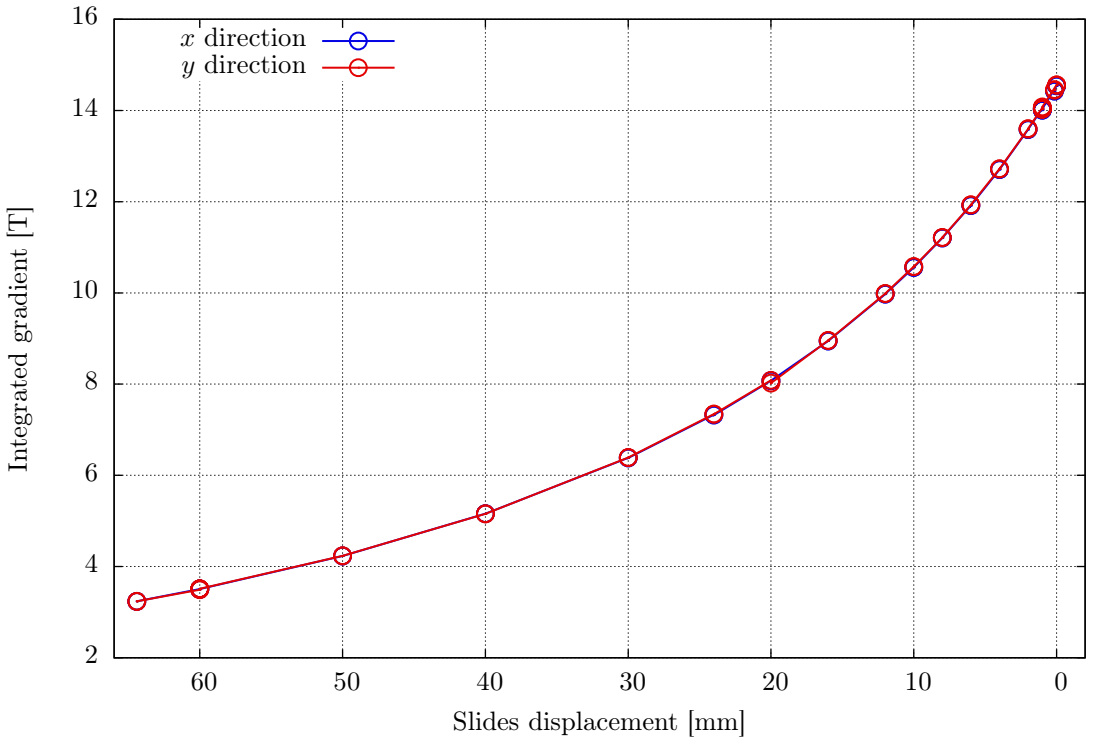

Figure 3: characteristic curve of the CLIC DBQ-PM.

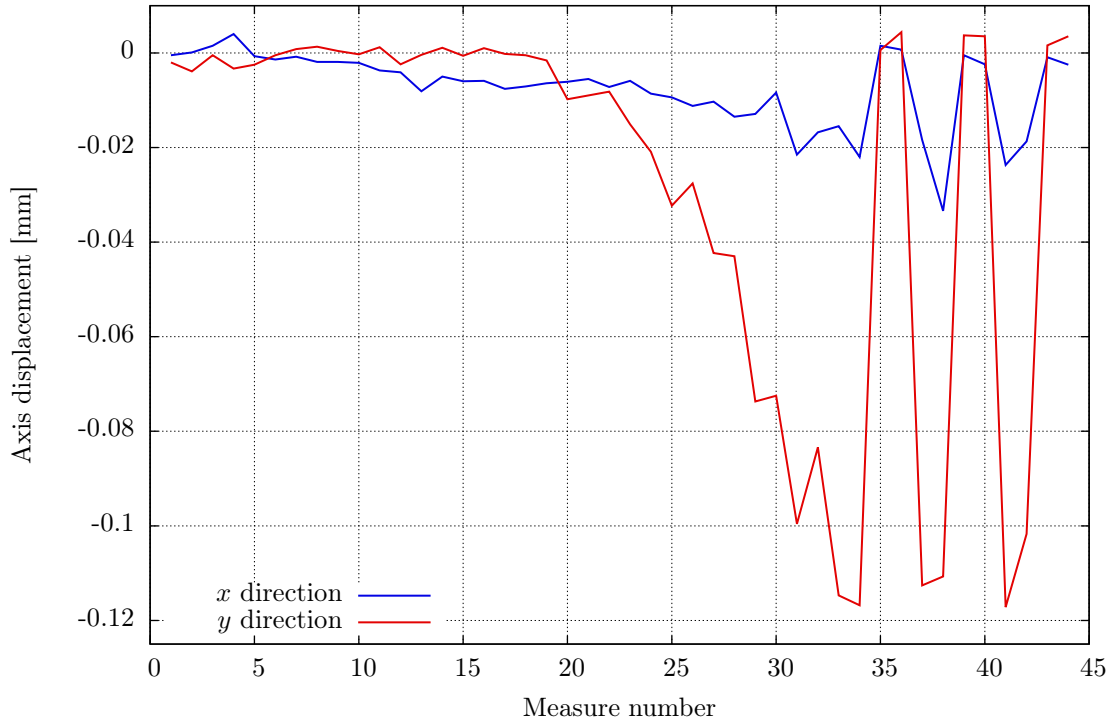

Figure 4: magnetic axis displacement in x and y directions.

gradient plot is evident, suggesting a strong correlation between operating gradient and axis position. While the range between 14.5 T and 10 T appears to be relatively stable, the one between 10 T and 4 T shows considerable displacement, especially in the y direction, in which the axis moves more than 100 µm (the repeatability of the measurements decreases at lower gradients, due to the weakening of the signal seen by the integrator). Moreover, this displacement appears to be repeatable, as the axis comes back to its original position each time that the maximum gradient is reached again, and travels back to the displaced position when the minimum gradient is imposed.
This behaviour requires further investigation, as the CLIC drive beam performances depend strongly on the precision achievable in the positioning of the magnetic axes of the quadrupoles with respect to the beam line. In figures 5 and 6 the axis displacements are plotted in function of the integrated gradient and slide position, respectively. In both cases, a non linear relation is evident, but these plots cannot explain this phenomenon by themselves. This dependency is probably to attribute to two factors: a mechanical phenomenon, for which the two halves of the magnet are not moving as required or deformations occur in the yokes or in the poles; and a magnetic phenomenon, which requires particular attention. When this quadrupole works in the low gradient region, the air gap between the permanent magnet blocks and the iron poles is at its maximum. In this configuration there is a considerable amount of magnetic flux that escapes from the magnet, and such flux could assume a complex path depending by the ferromagnetic components that are placed close to the magnet core, like the motors, the gearings and

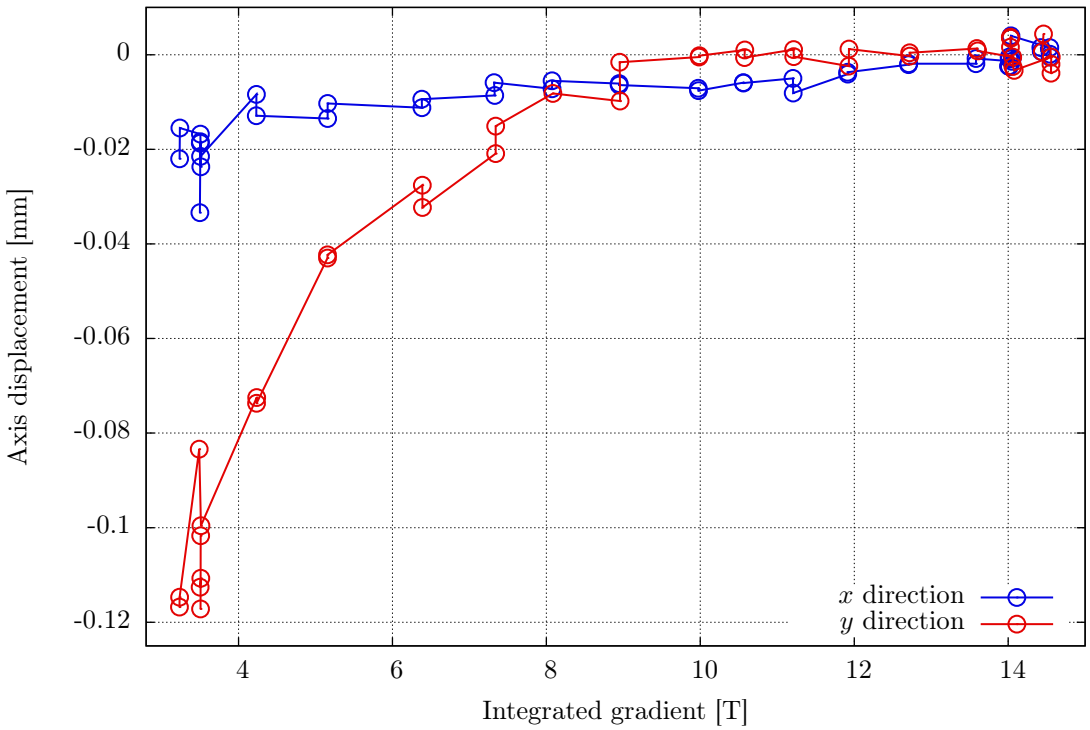

Figure 5: axis displacement versus integrated gradient.

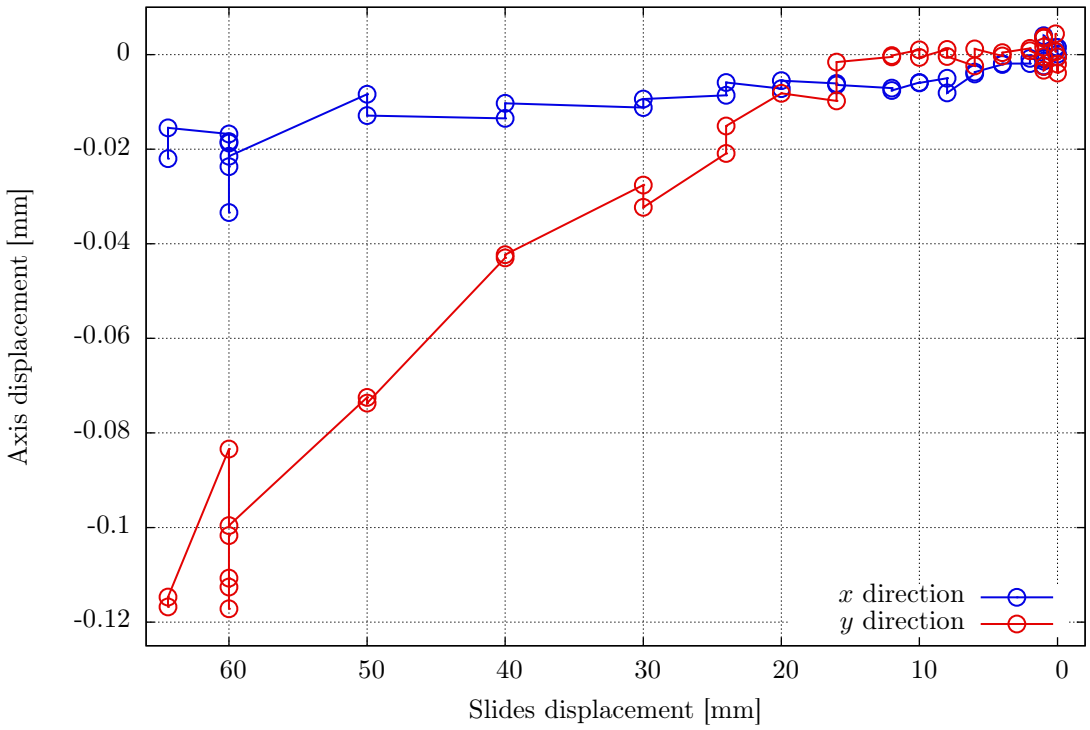

Figure 6: axis displacement versus slides displacement.

also the measuring equipment. This relatively big part of fringe field could affect the overall magnetic length, and the axis position as well, since the shape of the fringe field is hardly predictable when far from the magnet and close to other ferromagnetic components. This phenomenon could potentially affect also the quality of the measurements themselves.
In conclusion, after the result obtained in this first magnetic measurements, it was decided to focus on the mechanical aspects and send the magnet to the Metrology Laboratory, to perform precise measurements of the DBQ-PM components movements and deformations at different operating gradients.

3. Mechanical measurements

These measurements aimed to check the correct slide positioning at different operating gradients, and also to discover if unexpected deformations of the DBQ-PM structure could occur. However the magnet has a relevant fringe field, which was considered high enough to interfere with the sensitive elements of the measuring machines.
For this reason two different measuring machines were used: the first is expected to be less affected by the magnetic stray field, while the second machine is more precise, and can be programmed to measure arrays of points along complex paths, with the disadvantage of being more sensitive to the magnetic field. Both machines are located in the CERN Metrology Laboratory, in Building 100, which provides a stable environment in terms of temperature and humidity. A measurement report [1] is also provided by the colleagues of the EN-MME.

3.1. The first machine

The first machine to be used was the `VERTICAL3 TRIMOS`. Such device consists in a vertical tower capable of performing vertical measurements of length. This tower levitates over air cushions on a level granite block, and can be positioned by hand on the measuring spot. The resolution of such instrument is 1 µm, with a error of ±5 µm, however, since the sensitive element is positioned by hand in the horizontal plane, it is not guaranteed that the measuring points is exactly the same during consequent measurements. To reduce the error relative to this uncertainty, a small statistic over three acquisitions is performed for every single measuring point.
Figure 7 shows the DBQ-PM next to the measuring instrument. The red arrows represent the points that were used as reference to level the magnet, while the blue arrows represent the adjustable supports. Figure 8 shows the points that were measured. As a convention, the first digit stands for the upper slide (2) or the lower slide (1); while the second digit ranges from 0 to 5, for a total of six points measured on each slide.

3.1.1. The first cycle

The cycle followed during this measure started from the maximum gradient configuration, achieved by moving the permanent magnet slides towards the poles, until the

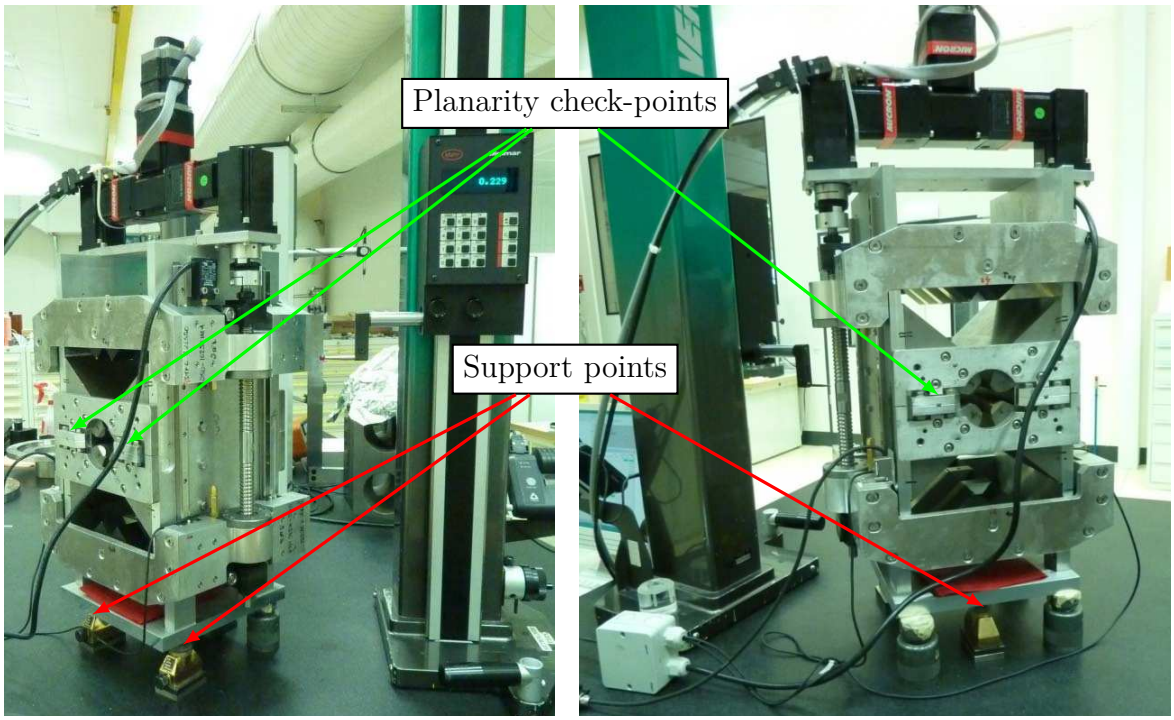

Figure 7: the quadrupole and the VERTICAL3 machine.

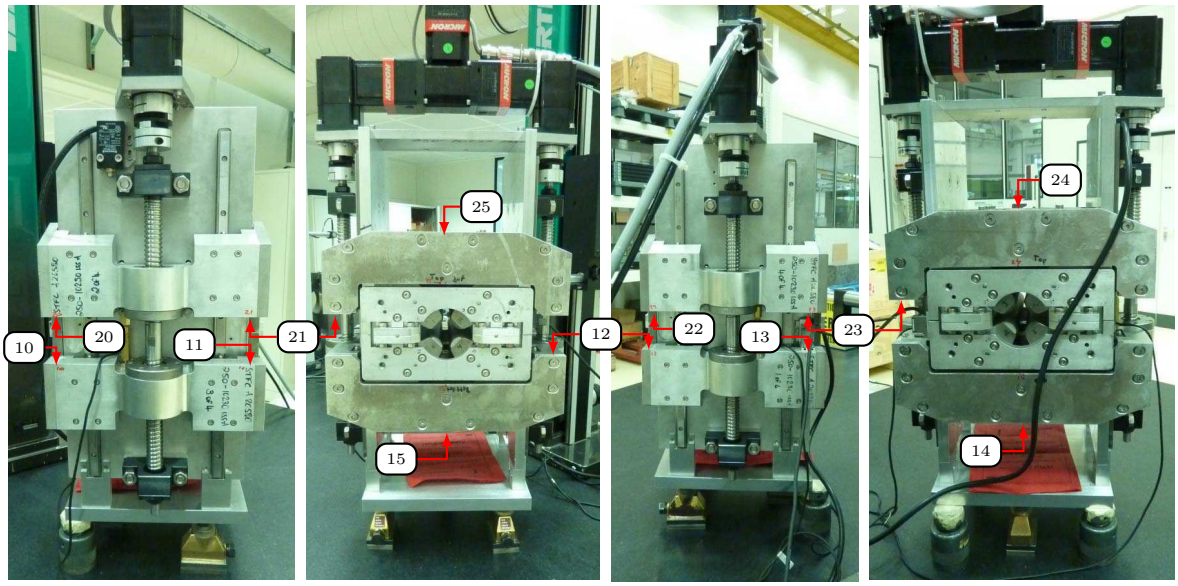

Figure 8: the measuring points on the quadrupole slides.

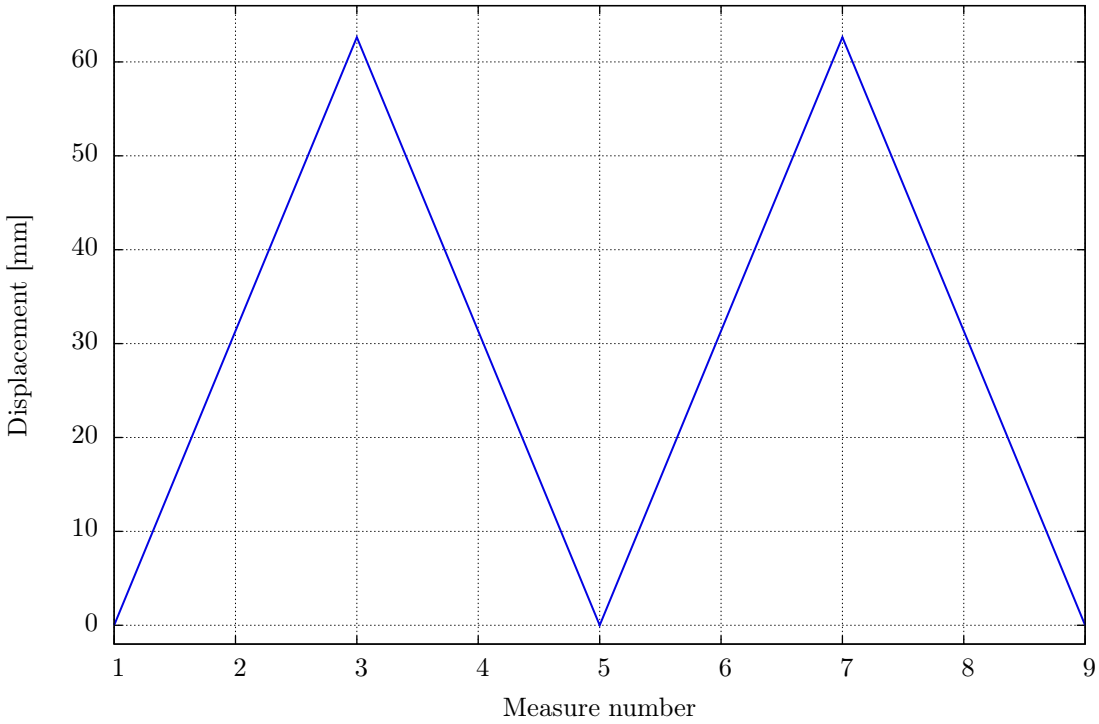

Figure 9: linear encoder readout during the measurement cycle.

intervention of the end-switch. From this point, the slides were moved away from the poles by 62.6 mm, then back to the poles; and finally away and back for a second time, as represented in figure 9. Intermediate measurements were taken each time the values of 0 mm 31.3 mm and 62.6 mm were reached.

3.1.2. The second cycle

After the measurement on the full operational scale, it was decided to focus on a small range close to the maximum gradient configuration. For this second cycle, the end-switch was removed and the stepper motor controlling the slides was powered off, so that the moving parts were free to get in contact with the poles. After this zeroing, the motor was powered on again and the slides were moved by steps of 1 mm away from the poles, while measuring the position of the same points of the previous cycle. In total 5 slides positions were measured, including the one in contact with the poles.

3.1.3. The third cycle

Finally, to compare the readouts of the angular encoder on the stepper motor and the linear encoder on the slide, a long series of 33 measurements was performed. In this last case the `VERTICAL3` machine was not used.

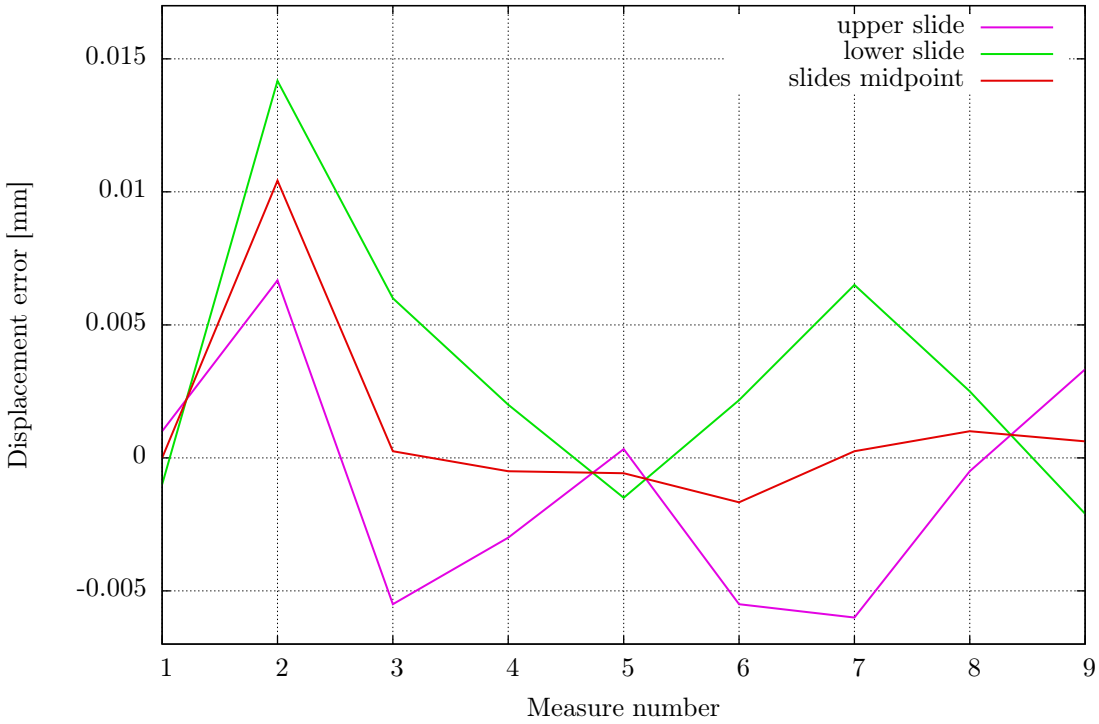

Figure 10: error on the average displacements of the slides.

3.2. Results of the first machine measurements

The first cycle of measurements shows two important results. The first information, shown in figure 10, concerns the error on the average position of the two slides, and their symmetric movement about a theoretical midpoint. Such midpoint in particular looks very stable in the vertical direction, and most importantly does not show any systematic correlation with the slides positions. This leads to exclude any correlation between the magnetic axis displacement and an hypothetical asymmetry in the slides movement.

The second information obtained with the first cycle of measurements concerns the deformation of the slides: the difference between the position of a single point and the average of all the points belonging to the same slide are plotted in figures 11 and 12, respectively for the upper and lower slides.

From these plots it can be noticed how the slides deform, as the middle points (numbers 14, 15, 24 and 25) show a difference that goes up to 0.1 mm with respect to the point that are on the corner (numbers 10, 11, 12, 13, 20, 21, 22 and 23).

Such deformation depends on the gradient intensity and can be interpreted as a flexural deformation of the whole slide, which is higher at higher gradients, when the center points of the slides come closer to the poles than the points of the corners.

3.2.1. Results of the second cycle

The second cycle confirms in a smaller scale the same flexural tendency shown before, but also points out that when the slides enter in contact with the poles, their position is no longer coherent with their usual path. This "self-adjustment" was expected, as the equilibrium of the slides change completely due to new surfaces that enter in contact for the first time; still these measurements gave an estimate of the value of the displacements caused by this contact.
Figures 13 and 14 show the results of the second cycle of measurements, normalized with respect to the second measuring point, which is the first one to be measured after the slides detach from the poles.

3.2.2. Results of the third cycle

Finally, in the third cycle it was calculated the error between the angular encoder readout, multiplied by the gear ratio to obtain a linear displacement, and the readout of the linear encoder.
The result is plotted in figure 15, and this error shows a clear correlation with the slide position. It is to be noticed that the error is defined as zero for the first measure (slides in contact with the poles) and it tends to return to this value when the slides are moved far enough, confirming that in the high gradient operating range the magnetic forces have a strong impact on the mechanics of this quadrupole assembly.

3.3. The second machine

The second machine used was a 3D measuring station model `Inspector Maxi 900v`, made by Olivetti. Figure 16 shows the DBQ-PM positioned on this measuring station. The error of this machine is within $\pm 3\,\mu m$, but in this case there were concerns about the possibility to operate it in presence of strong magnetic fields. For this reason the machine was firstly calibrated using a reference prism, and then the same prism was measured again, after installing the DBQ-PM close to it, in the configuration that gives maximum fringe field. The second measurement was not disturbed by the field, therefore it was concluded that the magnetic field is not strong enough to perturb the results.

3.3.1. Measuring cycle

The DBQ-PM stepper motor was turned off and the slides were let free to touch the back surface of the poles, reaching the maximum gradient. After the contact occurred, the motor was powered again and the slides were moved from 0 mm to 10 mm, performing a full measure every mm, for a total of 11 measurements. Later, this whole procedure was repeated to measure 5 points, going from 0 mm to 60 mm by steps of 15 mm; and finally 4 more measure were taken going from 0 mm to 60 mm by 20 mm. The interesting thing about this machine is that it allowed to measure not only the same points that were measured by the vertical machine, but also several points belonging to the pole tips. These points were defined by giving the CAD model of the DBQ-PM as an input to the

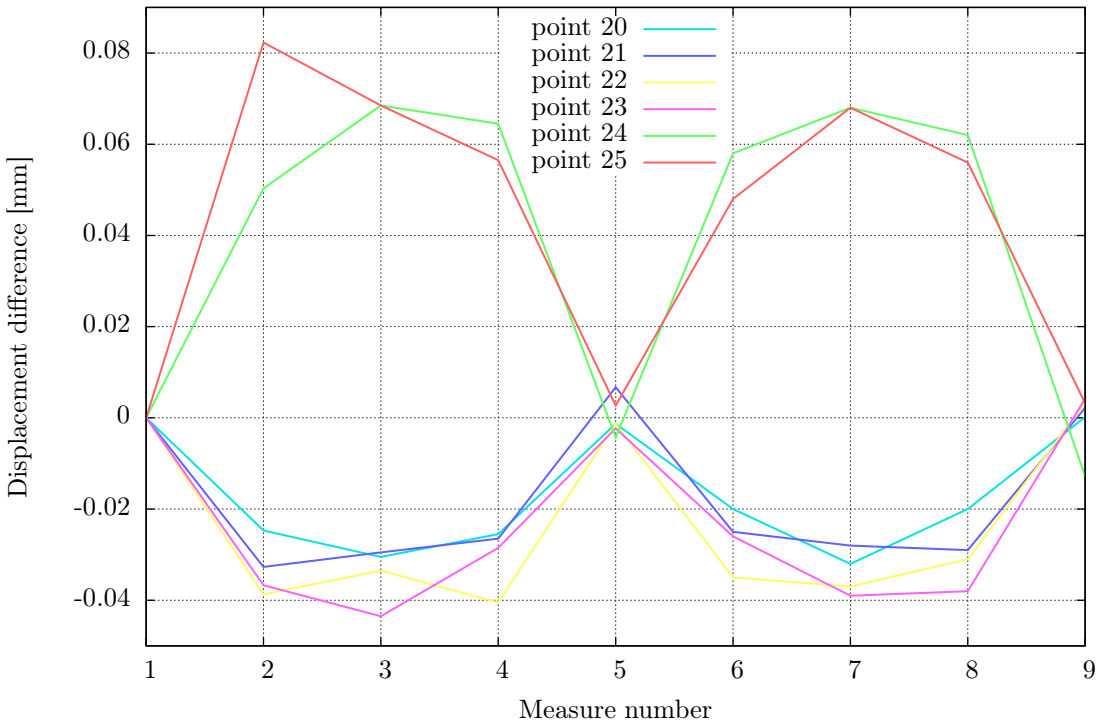

Figure 11: difference between local and average displacement, upper slide, first cycle.

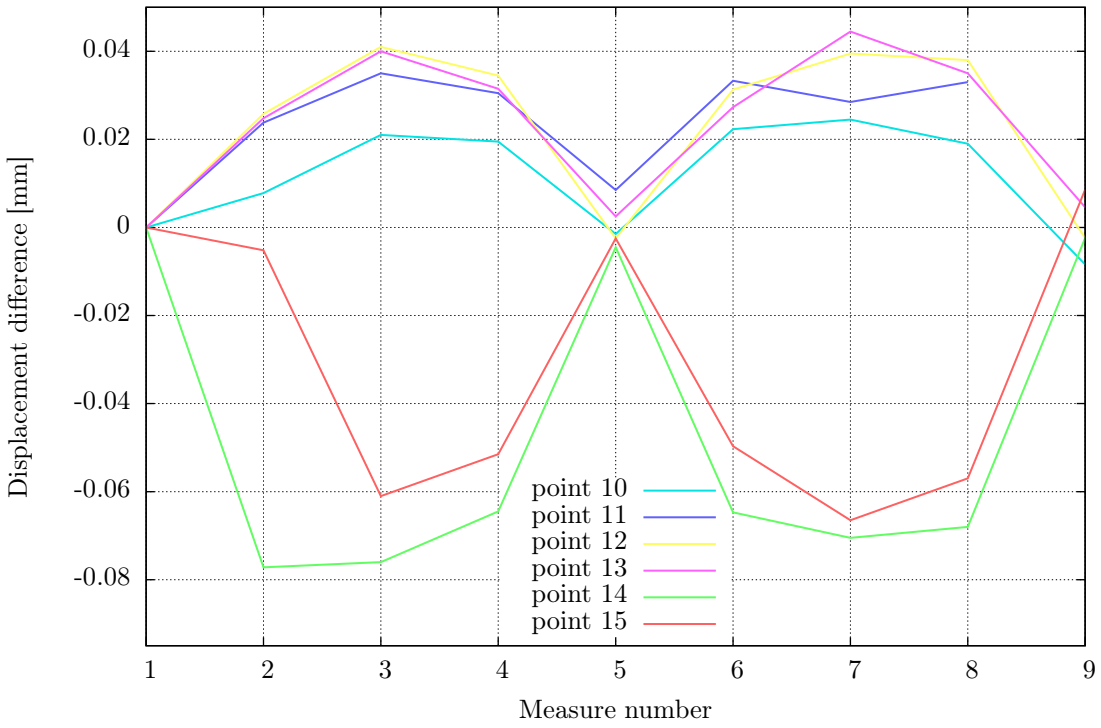

Figure 12: difference between local and average displacement, lower slide, first cycle.

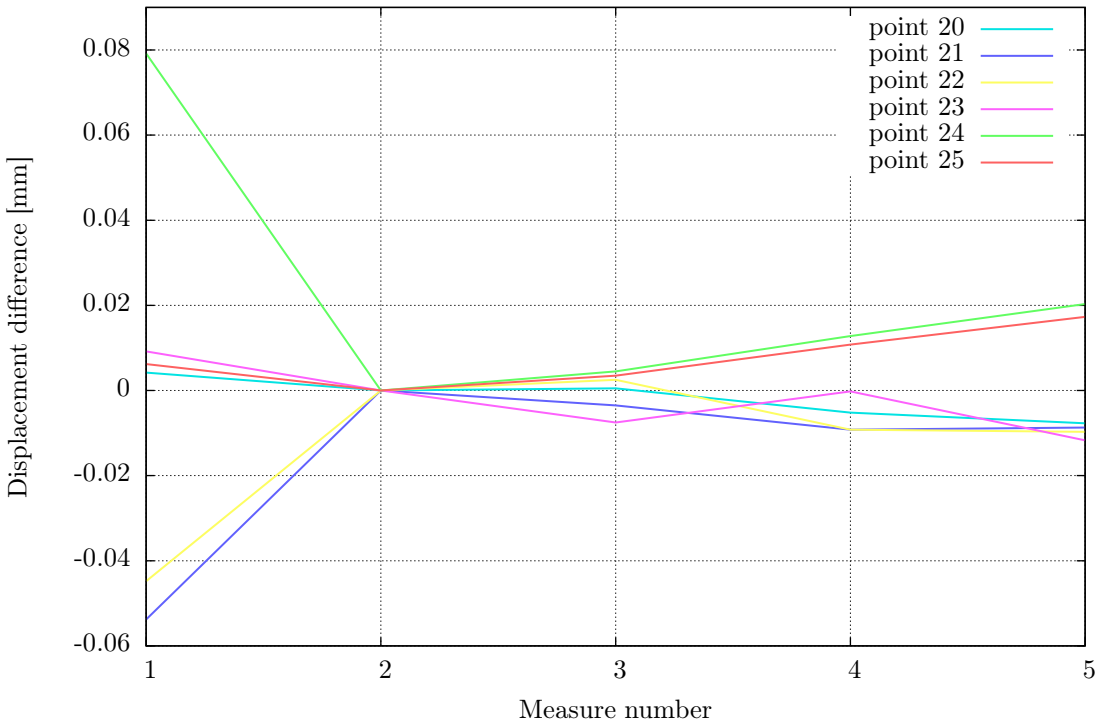

Figure 13: difference between local and average displacement, upper slide, second cycle.

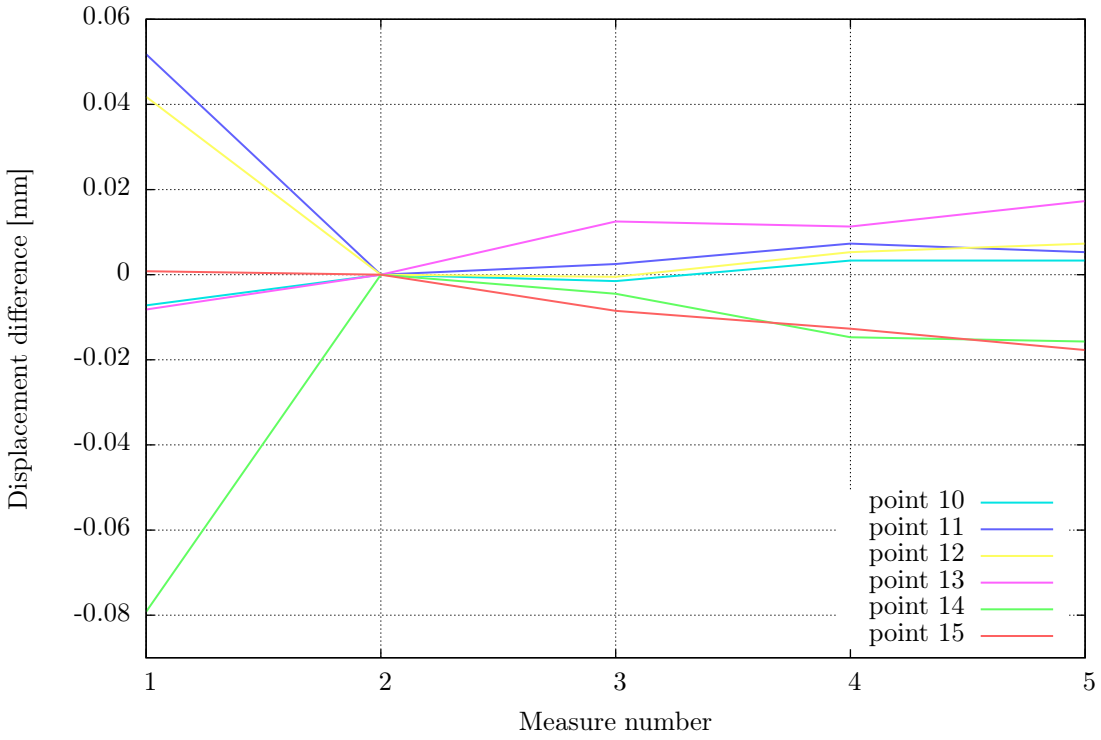

Figure 14: difference between local and average displacement, lower slide, second cycle.

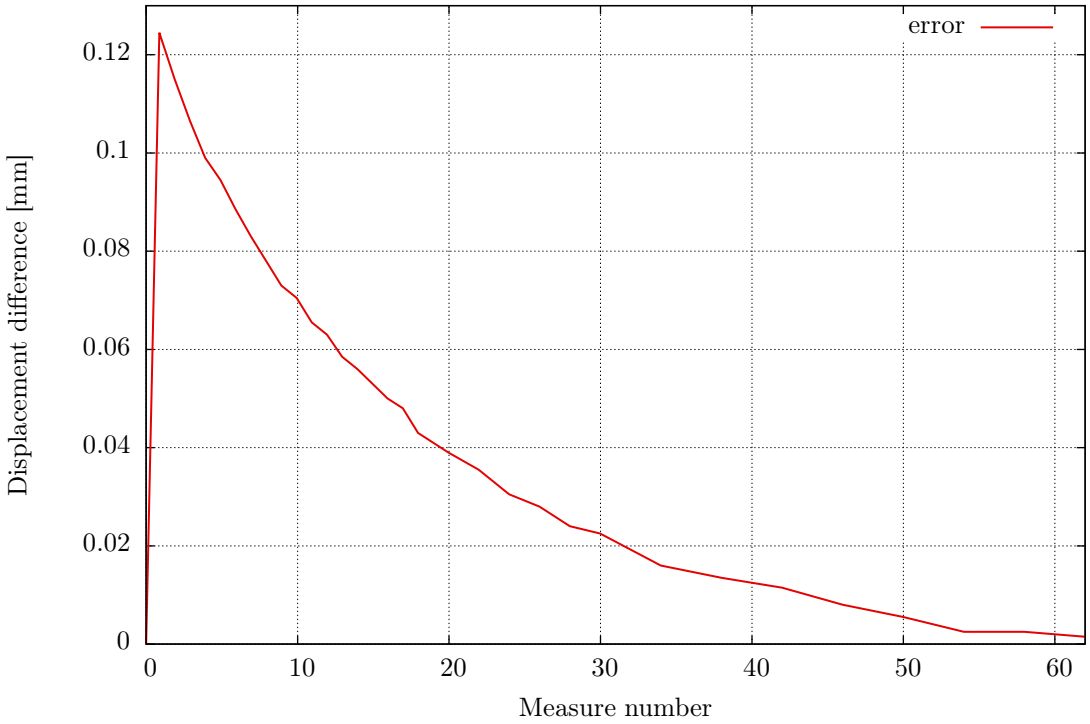

Figure 15: error between encoder reading and expected slide displacement.

machine.
A fitting hyperbola, compatible with the theoretical pole profile, was then calculated by the machine, permitting to find a *geometric center* based on the coordinates of the acquired points. This routine was performed once per each side of the magnet.

3.4. Results analysis

The first interesting result is about the poles center, that was measured for the first time in this occasion. Figure 17 shows a plot of the x and y displacement of the center, measured at the two extremities of the DBQ-PM, called "$z+$ face" and "$z-$ face". As usual z is along the beam axis, y is vertical and x is horizontal.
From this plot is evident that especially in the y direction the displacement of the poles center can be correlated with the slide position, and then to the operating gradient.
Moreover, the movement of the points belonging to the slides confirmed the results obtained with the vertical machine. Figures 20 and 21 show the difference between the position of each point with respect to the average, for the upper and lower slide, respectively. In the second case it is especially evident how the midpoints end up in a position that is almost 0.1 mm far from the position reached by the points in the corners when the slide is moved by 60 mm.
In the upper slide this plot is different, suggesting a tilt or a torsion of the slide itself.

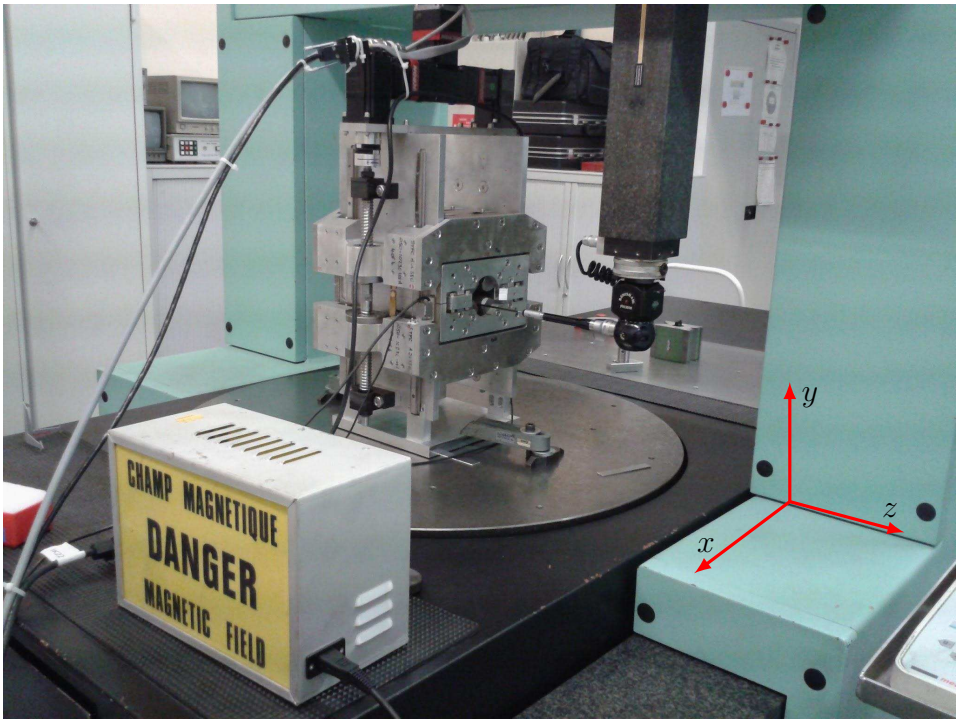

Figure 16: the magnet on the Olivetti Inspector Maxi 900v.

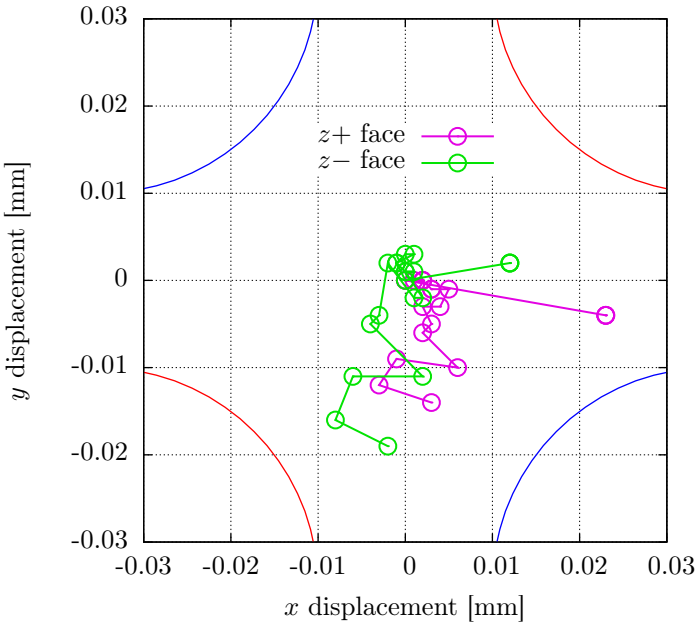

Figure 17: pole center position in the x–y plane (poles *not* to scale).

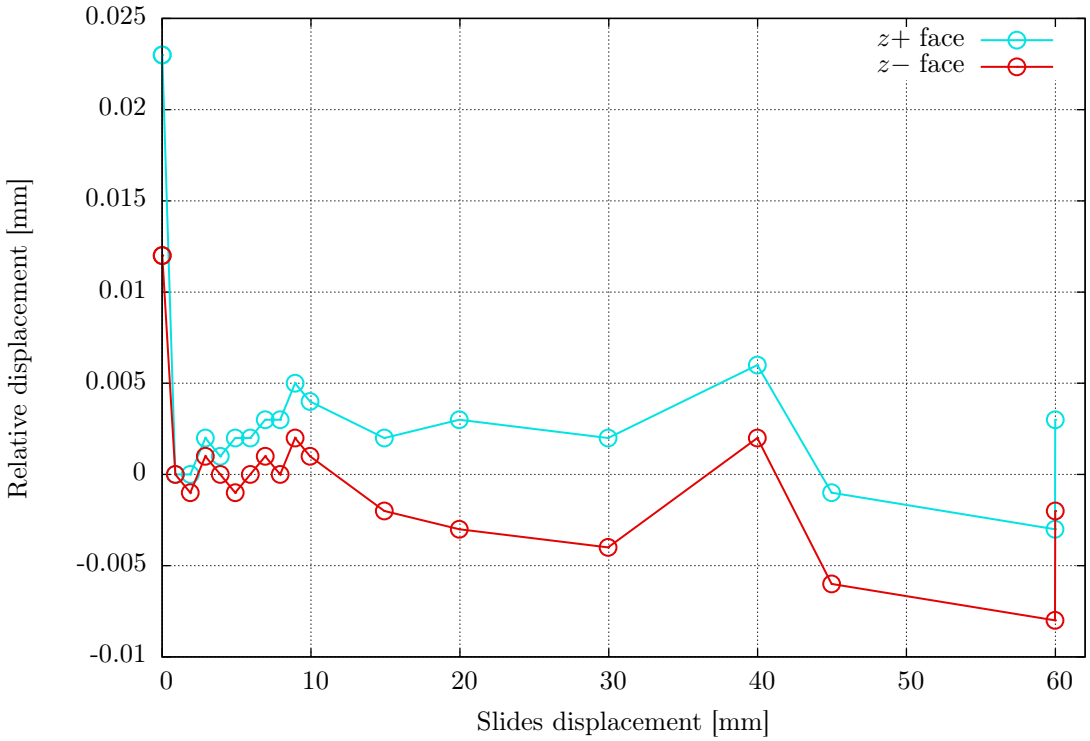

Figure 18: pole center displacement in the x direction.

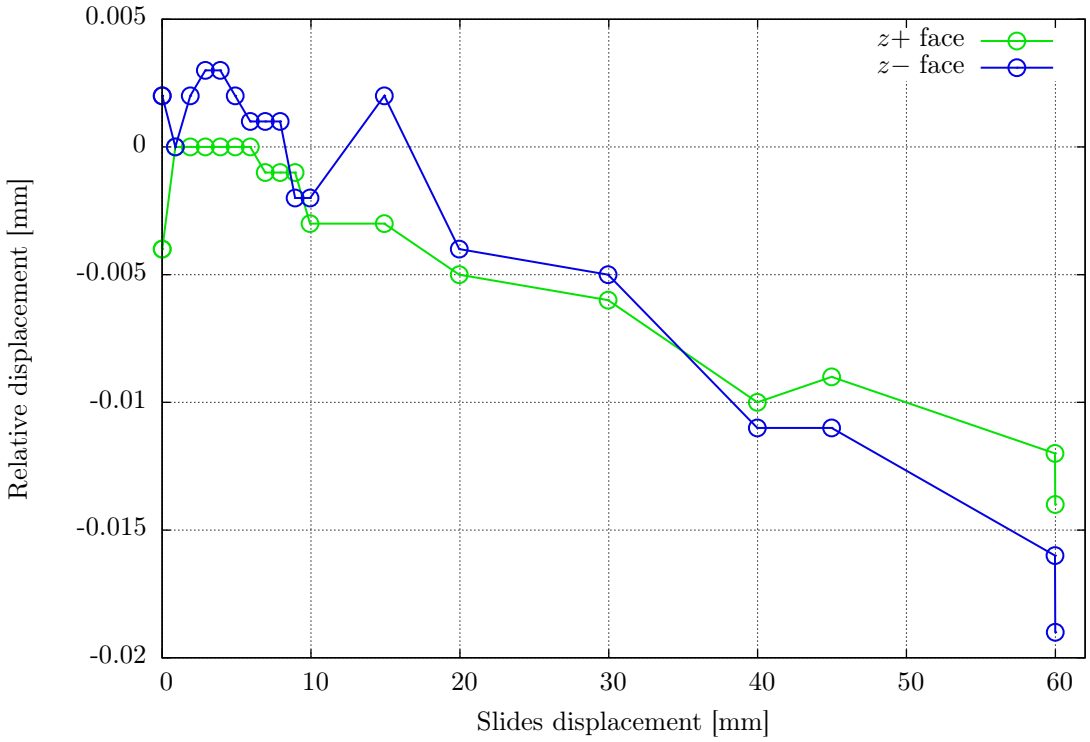

Figure 19: pole center displacement in the y direction.

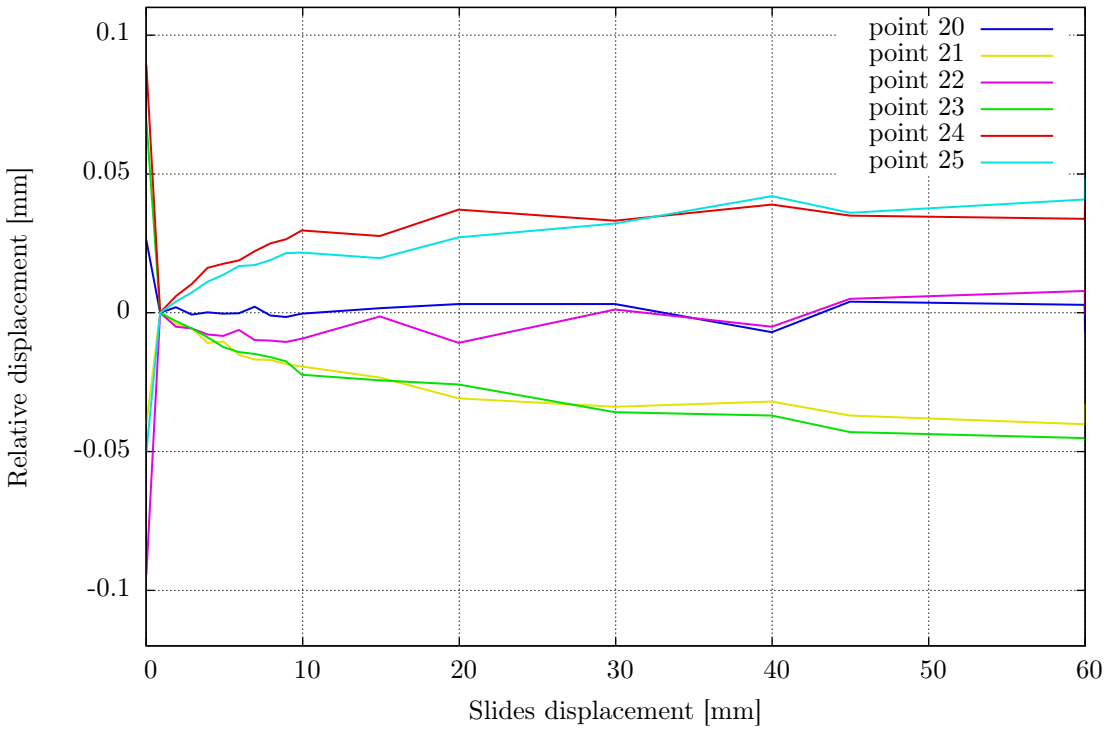

Figure 20: difference between local and average displacement, upper slide.

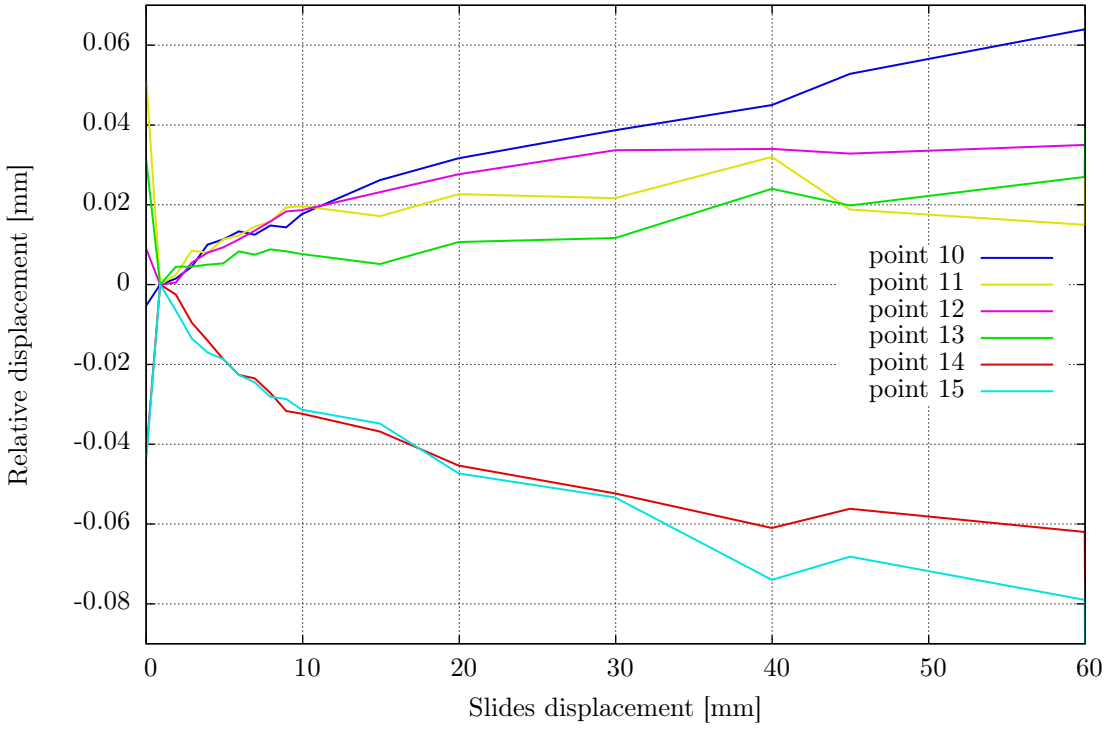

Figure 21: difference between local and average displacement, lower slide.

4. Conclusions

From the magnetic point of view, the maximum integrated gradient and the characteristic curve were measured and considered satisfactory. The field quality is not yet measured, due to unavailability of a suitable rotating coil measuring system. The displacement of the magnetic axis however appears to be higher than expected, and this aspect requires to be better investigated and corrected.
Considering that the magnet was always measured at a stable temperature, the movements of the magnetic axis can be attributed to three different causes:

Asymmetries in the ferromagnetic ancillary devices: this includes all the ferromagnetic masses close to the DBQ-PM that could play a relevant role in presence of strong fringing field, by creating complex paths of magnetic flux and displace the position of the magnetic axis.

Asymmetries and inhomogeneities in the materials: eventual defects could play a role in the less saturated (lower gradient) operational range.

Mechanical error or compliances: eventual asymmetric movements of the DBQ-PM parts during the setting operation would lead to asymmetries in the magnetic field gradient.

Since the first two points could not be investigated without disassembling the magnet, it was decided to focus on the mechanical performances of the DBQ-PM, and a series of mechanical measurements was performed.
The results pointed out a remarkable precision achieved in the slides movements, and most importantly a consistent symmetry of these movements with respect to the horizontal midplane of the magnet, suggesting to exclude the hypothesis of a role of the slides in the displacement of the magnetic axis. The slides however deformed more than expected, and the strong magnetic forces are supposed to induce an additional non linearity in the slides position controls when working at high gradients.
On the other hand, movements of the order of tens of micrometers were observed at the level of the poles, constituting a potential cause of the movement of the magnetic axis.

5. Acknowledgements

The authors express their sincere thanks to: Jim Clarke, Norbert Collomb and Ben Shepherd from Daresbury Lab., Juan Garcia Perez from CERN TE-MSC/MM Section, Lilian Philippe Remandet and Jean Philippe Rigaud from CERN EN-MME/MM Section, and Guido Sterbini from the CERN BE/ABP Group.

References

[1] J. P. Rigaud. CLIC PMQ top level assembly, presentation of the metrology results. Tech. Rep. EDMS nr. 1253783, CERN, Geneva, 2012.

Appendix A Magnetic measurements results

Measure number	integrated grad. x [T]	axis disp. x [mm]	integrated grad. y [T]	axis disp. y [mm]	slides disp. [mm]
1	14.544	-0.001	14.557	-0.002	0.000
2	14.544	0.000	14.556	-0.004	0.000
3	14.541	0.002	4.560	-0.001	0.000
4	14.037	0.004	14.079	-0.003	1.000
5	14.054	-0.001	14.061	-0.003	1.000
6	14.046	-0.001	14.059	-0.001	1.000
7	13.583	-0.001	13.603	0.001	2.000
8	13.581	-0.002	13.592	0.001	2.000
9	12.707	-0.002	12.719	0.000	4.000
10	12.705	-0.002	12.722	0.000	4.000
11	11.914	-0.004	11.932	0.001	6.000
12	11.916	-0.004	11.930	-0.002	6.000
13	11.207	-0.008	11.214	0.000	8.000
14	11.204	-0.005	11.213	0.001	8.000
15	10.562	-0.006	10.574	-0.001	10.000
16	10.559	-0.006	10.578	0.001	10.000
17	9.977	-0.008	9.987	0.000	12.000
18	9.973	-0.007	9.983	-0.001	12.000
19	8.945	-0.006	8.953	-0.002	16.000
20	8.947	-0.006	8.958	-0.010	16.000
21	8.075	-0.006	8.021	n\a	20.000
22	8.075	-0.007	8.084	-0.008	20.000
23	7.321	-0.006	7.342	-0.015	24.000
24	7.329	-0.009	7.342	-0.021	24.000
25	6.382	-0.009	6.391	-0.032	30.000
26	6.383	-0.011	6.389	-0.028	30.000
27	5.158	-0.010	5.156	-0.042	40.000
28	5.158	-0.014	5.157	-0.043	40.000
29	4.231	-0.013	4.234	-0.074	50.000
30	4.233	-0.008	4.236	-0.073	50.000
31	3.507	-0.022	3.511	-0.100	60.000
32	3.506	-0.017	3.490	-0.083	60.000
33	3.238	-0.016	3.236	-0.115	64.412
34	3.235	-0.022	3.234	-0.117	64.412
35	14.425	0.002	14.444	0.001	0.146
36	14.430	0.001	14.460	0.004	0.146
37	3.505	-0.018	3.502	-0.113	60.000
38	3.498	-0.033	3.510	-0.111	60.000
39	14.012	-0.001	14.028	0.004	1.000
40	14.004	-0.002	14.035	0.004	1.000
41	3.510	-0.024	3.507	-0.117	60.000
42	3.503	-0.019	3.508	-0.102	60.000
43	14.015	-0.001	14.030	0.002	1.000
44	14.017	-0.003	14.030	0.004	1.000

Table 1: stretched wire measurements listing.

Appendix B Mechanical measurements results

Measure number	point 20	point 21	point 22	point 23	point 24	point 25
1 (zeroing)	0.000	0.000	0.000	0.000	0.000	0.000
2	31.337	31.329	31.323	31.325	31.412	31.444
3	62.592	62.593	62.589	62.579	62.691	62.691
4	31.331	31.330	31.316	31.328	31.421	31.413
5	-0.003	0.005	-0.003	-0.004	-0.006	0.001
6	31.329	31.324	31.314	31.323	31.407	31.397
7	62.589	62.593	62.584	62.582	62.689	62.689
8	31.339	31.330	31.328	31.321	31.421	31.415
9	0.000	0.002	0.003	0.004	-0.013	0.003
1 (zeroing)	0.000	0.000	0.000	0.000	0.000	0.000
2	0.933	0.991	0.982	0.928	0.858	0.931
3	1.944	1.998	1.995	1.931	1.873	1.945
4	2.947	3.001	2.992	2.947	2.890	2.961
5	3.952	4.009	3.999	3.943	3.905	3.975

Table 2: displacement of the points on the upper slide in mm.

Measure number	point 10	point 11	point 12	point 13	point 14	point 15
1 (zeroing)	0.000	0.000	0.000	0.000	0.000	0.000
2	-31.333	-31.317	-31.315	-31.316	-31.418	-31.346
3	-62.601	-62.587	-62.581	-62.582	-62.698	-62.683
4	-31.338	-31.327	-31.323	-31.326	-31.422	-31.409
5	-0.001	0.009	-0.002	0.003	-0.004	-0.002
6	-31.330	-31.319	-31.321	-31.325	-31.417	-31.402
7	-62.596	-62.592	-62.581	-62.576	-62.691	-62.687
8	-31.338	-31.324	-31.319	-31.322	-31.425	-31.414
9	-0.007	-58.750[1]	-0.001	0.006	-0.001	0.010
1 (zeroing)	0.000	0.000	0.000	0.000	0.000	0.000
2	-0.934	-0.993	-0.983	-0.933	-0.862	-0.942
3	-1.945	-2.000	-1.993	-1.930	-1.876	-1.960
4	-2.948	-3.003	-2.995	-2.939	-2.894	-2.972
5	-3.955	-4.012	-4.000	-3.940	-3.902	-3.984

[1] this value is an error and it was discarded in the analyses

Table 3: displacement of the points on the lower slide in mm.

Measure number	angular encoder	linear encoder [mm]	expected value [mm]	error [mm]
1	0	0.000	0	0.000
2	4000	0.876	1	0.125
3	8000	1.885	2	0.115
4	12000	2.894	3	0.107
5	16000	3.901	4	0.099
6	20000	4.906	5	0.095
7	24000	5.912	6	0.088
8	28000	6.917	7	0.083
9	32000	7.922	8	0.078
10	36000	8.927	9	0.073
11	40000	9.930	10	0.070
12	44000	10.935	11	0.066
13	48000	11.937	12	0.063
14	52000	12.942	13	0.059
15	56000	13.944	14	0.056
16	60000	14.947	15	0.053
17	64000	15.950	16	0.050
18	68000	16.952	17	0.048
19	72000	17.957	18	0.043
20	80000	19.961	20	0.039
21	88000	21.965	22	0.035
22	96000	23.970	24	0.031
23	104000	25.972	26	0.028
24	112000	27.976	28	0.024
25	120000	29.978	30	0.023
26	136000	33.984	34	0.016
27	152000	37.987	38	0.014
28	168000	41.989	42	0.011
29	184000	45.992	46	0.008
30	200000	49.995	50	0.005
31	216000	53.998	54	0.002
32	232000	57.998	58	0.002
33	248000	61.999	62	0.002

Table 4: encoder readout comparison.

Appendix C 3D Mechanical measurements results

Angular encoder	linear encoder	point 20	point 21	point 22	point 23	point 24	point 25
-1	-0.006	0.000	0.000	0.000	0.000	0.000	0.000
3999	0.884	-0.026	0.040	0.094	-0.069	-0.089	0.050
7999	1.893	-0.024	0.036	0.089	-0.072	-0.083	0.054
11999	2.901	-0.027	0.034	0.088	-0.075	-0.079	0.057
15999	3.909	-0.026	0.029	0.086	-0.078	-0.073	0.061
19999	4.913	-0.026	0.030	0.086	-0.081	-0.071	0.064
23999	5.919	-0.026	0.025	0.088	-0.083	-0.070	0.067
27999	6.925	-0.024	0.023	0.084	-0.084	-0.067	0.067
31999	7.930	-0.027	0.023	0.084	-0.085	-0.064	0.069
35999	8.935	-0.027	0.021	0.083	-0.086	-0.062	0.071
39999	9.937	-0.026	0.021	0.085	-0.091	-0.059	0.072
4	0.008	0.000	0.000	0.000	0.000	0.000	0.000
60004	14.928	-0.024	0.017	0.093	-0.093	-0.061	0.070
120004	29.958	-0.023	0.006	0.095	-0.105	-0.056	0.082
180004	44.971	-0.022	0.003	0.099	-0.112	-0.054	0.086
240004	59.978	-0.023	0.000	0.102	-0.114	-0.055	0.091
0	0.000	0.000	0.000	0.000	0.000	0.000	0.000
80000	19.957	-0.023	0.009	0.083	-0.095	-0.052	0.077
160000	39.980	-0.033	0.008	0.089	-0.106	-0.050	0.092
240000	59.990	-0.033	0.007	0.093	-0.116	-0.050	0.098

Table 5: displacement of the points on the upper slide in mm.

Angular encoder	linear encoder	point 10	point 11	point 12	point 13	point 14	point 15
-1	-0.006	0.000	0.000	0.000	0.000	0.000	0.000
3999	0.884	0.005	-0.051	-0.009	-0.031	0.042	0.043
7999	1.893	0.007	-0.048	-0.008	-0.026	0.040	0.037
11999	2.901	0.010	-0.042	-0.003	-0.026	0.033	0.030
15999	3.909	0.015	-0.043	-0.001	-0.026	0.028	0.026
19999	4.913	0.016	-0.039	0.000	-0.025	0.023	0.024
23999	5.919	0.018	-0.038	0.002	-0.022	0.019	0.020
27999	6.925	0.018	-0.036	0.005	-0.023	0.019	0.019
31999	7.930	0.020	-0.035	0.007	-0.022	0.015	0.015
35999	8.935	0.019	-0.031	0.009	-0.022	0.010	0.014
39999	9.937	0.023	-0.031	0.010	-0.023	0.010	0.012
4	0.008	0.000	0.000	0.000	0.000	0.000	0.000
60004	14.928	0.031	-0.034	0.014	-0.026	0.005	0.008
120004	29.958	0.044	-0.029	0.025	-0.019	-0.010	-0.010
180004	44.971	0.058	-0.032	0.024	-0.011	-0.014	-0.025
240004	59.978	0.069	-0.036	0.026	-0.004	-0.020	-0.036
0	0.000	0.000	0.000	0.000	0.000	0.000	0.000
80000	19.957	0.037	-0.028	0.019	-0.02	-0.003	-0.004
160000	39.980	0.050	-0.019	0.025	-0.007	-0.019	-0.031
240000	59.990	0.066	-0.020	0.025	0.008	-0.032	-0.047

Table 6: displacement of the points on the lower slide in mm.

Angular encoder	linear encoder	$z+$ face x direction	$z+$ face y direction	$z-$ face x direction	$z-$ face y direction
-1	-0.006	0.023	-0.004	0.012	0.002
0	0.000	0.023	-0.004	0.012	0.002
4	0.008	0.023	-0.004	0.012	0.002
3999	0.884	0.000	0.000	0.000	0.000
7999	1.893	0.000	0.000	-0.001	0.002
11999	2.901	0.002	0.000	0.001	0.003
15999	3.909	0.001	0.000	0.000	0.003
19999	4.913	0.002	0.000	-0.001	0.002
23999	5.919	0.002	0.000	0.000	0.001
27999	6.925	0.003	-0.001	0.001	0.001
31999	7.930	0.003	-0.001	0.000	0.001
35999	8.935	0.005	-0.001	0.002	-0.002
39999	9.937	0.004	-0.003	0.001	-0.002
60004	14.928	0.002	-0.003	-0.002	0.002
80000	19.957	0.003	-0.005	-0.003	-0.004
120004	29.958	0.002	-0.006	-0.004	-0.005
160000	39.980	0.006	-0.010	0.002	-0.011
180004	44.971	-0.001	-0.009	-0.006	-0.011
240004	59.978	-0.003	-0.012	-0.008	-0.016
240000	59.990	0.003	-0.014	-0.002	-0.019

Table 7: displacement of the center in mm.